sciendo

DOI 10.2478/ama-2022-0014

acta mechanica et automatica, vol.16 no.2 (2022)

BEHAVIOUR OF A NON-NEWTONIAN FLUID IN A HELICAL TUBE UNDER THE INFLUENCE OF THERMAL BUOYANCY

Mohamed RAMLA[*], Houssem LAIDOUDI[**], Mohamed BOUZIT[**]

[*]Faculty of Physics, Oran University of Science and Technology - Mohamed Boudiaf,
BP 1505, El-Menaouer, Oran, 31000, Algeria
[**]Laboratory of Sciences and Marine Engineering, Faculty of Mechanical Engineering,
Oran University of Science and Technology - Mohamed Boudiaf, BP 1505, El-Menaouer, Oran, 31000, Algeria

ramla_med@yahoo.fr, houssem.laidoudi@univ-usto.dz, bouzit-mohamed@yahoo.fr

received 1 December 2021, revised 4 February 2022, accepted 7 February 2022

Abstract: This work is an evaluative study of heat transfer in the helical-type heat exchanger. The fluid used is non-Newtonian in nature and is defined by Oswald's model. The work was performed numerically by solving each of the Navier–Stokes equations and the energy equation using the package ANSYS-CFX. Following are the aspects that have been dealt with in this paper: the effects of thermal buoyancy, fluid nature and the tube shape on the heat transfer, and the fluid comportment. The interpretation of the obtained results was done by analyzing the isotherms and the streamlines. The mean values of the Nusselt number were also obtained in terms of the studied parameters. The results of this research enabled us to arrive at the following conclusion: the intensity of thermal buoyancy and the nature of the fluid affect the heat transfer distribution but keep the overall rate of heat transfer the same.

Key words: helical heat exchanger, mixed convection, forced convection, power-law fluids, Nusselt number

1. INTRODUCTION

The helical shape of tubes is one of the techniques used in many industrial applications, primarily heat exchangers. It is also used in the production of industrial food stuffs such as jam, chocolates and others. Because of the importance of this type of tubes, many researchers have devoted a set of works showing the behaviour of the fluid inside the tube and the effect of this behaviouron the quality of heat transfer.

[1] demonstrated the possibility of improving heat transfer within a spiral tube by creating columns within the inner walls of the tube. The fluid investigated in this research is of the non-Newtonian type mixed with Al_2O_3 nanoparticles. [2] numerically simulated the passage of nanofluids and studied the heat transfer within aspiral tube,which contained ribs. The study showed that the presence of ribs enhances heat transfer by 12%. [3] exploited the finite volume method to compute the heat transfer in a helical tube. The geometrical dimensions of the tube were designed for a micro-system. The work mainly examined the effect of velocity and the length of the helix's pitch on the thermal behaviour. Through this work, it was concluded that the helical length of the tube has an effect on the thermal activity. [4] presented an entire experimental work on the behaviour of a two-phase stream in a helical tube. The use of this type of two-phase stream increases the heat transfer coefficient by up to 20%. [5] worked on a multiple-row helical tube, with the purpose of deriving the correlation that shows the changes in heat transfer in terms of the elements acting on it. [6] studied the effect of an external current around a helical tube,which was used for heat transfer. It has been found that this type of tube reduced the dead zone in the back. [7] determined the correlation between the Nusselt number and the friction factor for helical tubes. The thermal transfer was forced convection. [8] submitted a detailed report on a study conducted on helical tubes specially used in the heat pump. This work explained in detail the thickness of the resulting ice in terms of the conditions used. [9] did experimental research on helical tubes, where in they compared the geometry of the tubes. The new proposed shape included a group of corrugates on the tube. The obtained results were compared with those from smooth-walled tubes, and an increase in heat transfer was observed. [10] used the analytical method to study the flow within a helical tube of circular cross-section. The point studied in this work was the shape of the bend. [11] replaced the circular cross-section of the tube with a square one. Their work also included a study on the heat transfer of the forced convection type. [12] proposed an optimal design of a helical exchanger that can beused for absorption processes. The research was performed numerically using the commercial code ANSYS-Fluent. [13] presented a work on helical pipes for the measurement of frictional pressure losses. The results of this work were obtained experimentally and numerically as well. [14] further presented experimental results on the use of helical tubes for measuring the rheological properties of a complex fluid.Various researchers [15-17] also performed experiments on the curved tube, which showed an unusual disturbance of the flow.

In addition, the helical shape has a very important streamline compared to direct barriers, and this has been confirmed by most recent studies [18-21]. It is used in the structure of the heat exchangers to enhance the cooling process.

[22] made geometrical changes to the cross-section of the helical tube, from a simple circular shape to an organised circular shape of internal protuberances. In addition to this, a nanofluid

DOI 10.2478/ama-2022-0014

was used. Al_2O_3 nanoparticles were added to the basic fluid (water). There was an enhancement of heat transfer when the volume fraction reached 0.5%. [23] studied the turbulent regime of a flow in helical heat exchangers. The K-epsilon model was used for the mobilisation of the regime. The cross-section of the tube was semicircular. The results showed that this type of cross-section is highly recommended. Further, [24] performed numerical research on the turbulent flow in a sector-by-sector type helical tube . It was concluded that the semicircular form of the cross-section is more efficient for application in heat exchangers. [25] conducted studies on a double-cooling thermal exchanger,which is used in advanced aero-engine. This work aimed to find the best design of the tube that increases the effectiveness of cooling of the air that passes around the tube. [26] also introduced a numerical study on the helical tube, where the external and internal impacts of thermal transition are based on conjugate thermal boundary layers. [27] numerically compared a new type of helical tube with a single U-tube for application in heat exchangers. It was found that the helical type is more efficient than the U-tube. [28] used SiO_2/water and Al_2O_3/water nanofluids in the helical tube of a thermal exchanger.The research examined the concentration of the nanoparticles and a few geometrical configurations of the tube. The results of the work were given in the form of a correlation that relates the Nusselt number to the parameters considered in the study.

Because this type of tube is very important in thermal applications, several new works have been published on this topic to explain the scientific view on it [29-35]. In general, the main objective of these studies is to research the geometrical shape that increases the value of heat transfer.

[36] conducted an analytical study on double-helical tubes to achieve the most effective heat transfer. The studied elements were the taper angle and the cross-section. [37] simulated the flow of Al_2O_3/water nanofluids in a helical tube to increase the thermal transfer. The results proved that the presence of nanoparticles enhances thermal transfer. [38] performed a numerical simulation of the flow around a helical tube. The tube contained fins of various geometric shapes.The results showed that the presence of these fins increases thermal transfer.

Through our observation of these previous works, it becomes clear to us that these types of tubes have efficiency in increasing heat transfer, completely different from that of straight tubes. Moreover, most studies focused on forced heat transfer only. Further, the fluids used either had simple behaviour or were nanofluids. There is a lack of work that combines helical tubes and the non-Newtonian behaviour of a fluid in the presence of thermal buoyancy,which produces mixed heat transfer. Therefore, our work is a three-dimensional numerical simulation of a complex fluid inside a helical tube, with thermal buoyancy acting in the opposite direction of the fluid movement. The items considered here are as follows: the flow velocity at the inlet of the tube, the power law index that determines the rheological nature of the fluid, the intensity of thermal buoyancy and the pitch between the loops of the helical tube.

2. DESCRIPTION OF STUDIED DOMAIN

The tube under consideration is shown in Fig. 1. The tube has a helical shape containing three rings. The gap (the pitch) between the rings is constant and is given by (*B*). The inner diameter of the tube is given by the index (*d*),while the diameter of the tube ring is given by (*D*). These geometrical values are given in the form of ratios represented in Tab. 1. The studied fluid enters the tube at a constant velocity and low temperature (T_{in}). The walls of the tube have a high and constant temperature value (T_w). The difference in temperature between the fluid and the walls of the tube leads to heat transfer between the hot side and the cold side. The fluid velocity is given by the Reynolds number. The thermal buoyancy force acts in the direction (*Z*). Its intensity is described by the value of the Richardson number (Ri).

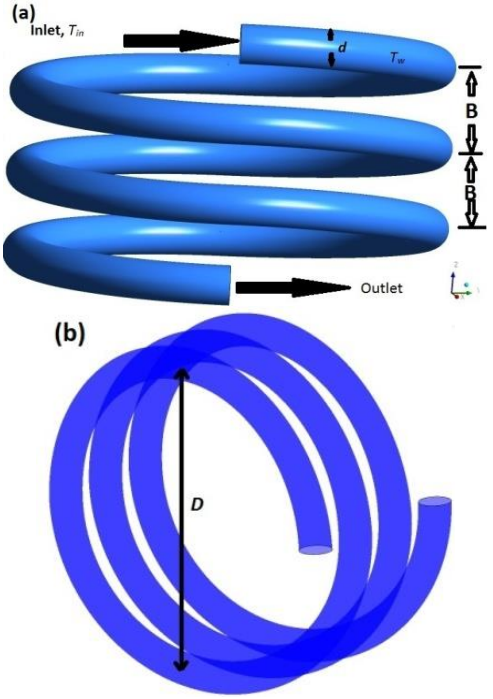

Fig. 1. Geometrical characteristics of the studied tube:
(a) first view; (b) second view (B, the pitch between the rings; d, inner diameter of the tube; D, diameter of the tube ring)

Tab. 1. Geometric rational values of the tube

Ratio	*d/D*	*B/D*
Value	0.1	0.2;0.4

3. MATHEMATICAL FORMULATIONS

In this section, we present the basic equations that must be solved numerically to obtain the numerical simulation of the desired study. These equations are as follows:

$$\frac{\partial U}{\partial X}+\frac{\partial V}{\partial Y}+\frac{\partial W}{\partial Z}=0 \quad (1)$$

$$U\frac{\partial U}{\partial X}+V\frac{\partial U}{\partial Y}+W\frac{\partial U}{\partial Z}=-\frac{\partial P}{\partial X}+\frac{1}{\mathrm{Re}}\left(\frac{\partial \tau^*_{xx}}{\partial X}+\frac{\partial \tau^*_{yx}}{\partial Y}+\frac{\partial \tau^*_{zx}}{\partial Z}\right) \quad (2)$$

$$U\frac{\partial V}{\partial X}+V\frac{\partial V}{\partial Y}+W\frac{\partial V}{\partial Z}=-\frac{\partial P}{\partial Y}+\frac{1}{\mathrm{Re}}\left(\frac{\partial \tau^*_{xy}}{\partial X}+\frac{\partial \tau^*_{yy}}{\partial Y}+\frac{\partial \tau^*_{zy}}{\partial Z}\right) \quad (3)$$

$$U\frac{\partial W}{\partial X}+V\frac{\partial W}{\partial Y}+W\frac{\partial W}{\partial Z}=-\frac{\partial P}{\partial Z}+\frac{1}{\mathrm{Re}}\left(\frac{\partial \tau^*_{xz}}{\partial X}+\frac{\partial \tau^*_{yz}}{\partial Y}+\frac{\partial \tau^*_{zz}}{\partial Z}\right)+\mathrm{Ri}\theta \quad (4)$$

$$U\frac{\partial \theta}{\partial X}+V\frac{\partial \theta}{\partial Y}+W\frac{\partial \theta}{\partial Z}=\frac{1}{\mathrm{Pr.Re}}\left(\frac{\partial^2\theta}{\partial X^2}+\frac{\partial^2\theta}{\partial Y^2}+\frac{\partial^2\theta}{\partial Z^2}\right) \quad (5)$$

The dimensionless quantities of the variable in the above equations are given as follows:

$$(X,Y,Z)=\frac{(x,y,z)}{d},(U,V,W)=\frac{(u,v,w)}{\mathrm{u_{in}}},P=\frac{p}{\rho \mathrm{u_{in}^2}},\theta=\frac{(T-T_{\mathrm{in}})}{(T_{\mathrm{w}}-T_{\mathrm{in}})} \quad (6)$$

$$\tau^*=\frac{\tau}{m(\frac{u_{in}}{d})^n} \quad (7)$$

The dimensionless numbers Re, Ri and Pr are given by the following expressions:

$$\mathrm{Re}=\frac{\rho(u_{in})^{2-n}d^n}{m} \quad (8)$$

$$\mathrm{Pr}=\frac{mc_p}{k\,(u_{in}/d)^{n-1}} \quad (9)$$

$$\mathrm{Ri}=\frac{\mathrm{Gr}}{\mathrm{Re}^2}=\frac{g\beta_T\Delta T d^3}{(u_{in})^2} \quad (10)$$

$$\mathrm{Gr}=g\beta_T\Delta T d^3[\frac{\rho}{m}(\frac{u_{in}}{d})^{1-n}]^2 \quad (11)$$

Through the Ostwald model, the viscosity is defined as follows:

$$\mu=m(\frac{I_2}{2})^{(\frac{n-1}{2})} \quad (12)$$

where I_2 is given by the following expression:

$$\frac{I_2}{2}=2(\frac{\partial u}{\partial x})^2+2(\frac{\partial v}{\partial y})^2+2(\frac{\partial w}{\partial z})^2+(\frac{\partial u}{\partial x}+\frac{\partial v}{\partial y}+\frac{\partial w}{\partial z})^2 \quad (13)$$

Generally, the fluid transfers heat in conductive and convective forms at the same time. The ratio between these two methods is determined by the Nusselt number, Nu. There is a local Nu number specific to each point in the analysed area, and there is an average value. These values of the Nusselt number are given respectively by the following two expressions:

$$\mathrm{Nu_L}=(\frac{\partial\theta}{\partial n_s})_{wall} \quad (14)$$

$$\mathrm{Nu}=\frac{1}{A}\int \mathrm{Nu_L}dA \quad (15)$$

where nsis the vector normal to the surface and *dA* is the elementary surface.

For every numerical work, a set of initial boundary conditions must be set for the simulation to occur. These boundary conditions are given as follows:

– At the inlet of the helical tube: cold temperature with uniform velocity:

$$U=0,V=1,W=0,\theta=0 \quad (16)$$

– On the tube walls: no-slip condition and hot temperature:

$$U=0,V=0,W=0,\theta=1 \quad (17)$$

– At the outlet tube: Neumann boundary condition is applied:

$$\frac{\partial U}{\partial X}=0,\frac{\partial V}{\partial X}=0,\frac{\partial W}{\partial X}=0,\frac{\partial\theta}{\partial X}=0 \quad (18)$$

4. NUMERICAL STEPS AND VALIDATION TEST

To achieve this simulation, several stages must be passed, which are arranged as follows: creating the grid for the studied domain, checking the effectiveness of this grid and checking the numerical methodology used for solving the mean equations.

The grid was created using Gambit. The grid cells were selected in quadratic form, as shown in Fig. 2. The grid contains 115.8000 elements. The effectiveness of the grid in finding the exact calculation depends mainly on the number of cells forming the entire grid. Three grids with different number of cells were created to calculate the Nu number for each case, so that the number doubles each time. The values of the elements together with the results of the calculation are shown in Tab. 2. The results are calculated for n = 1, Re = 100, Pr = 50 and Ri = 0. It is noted from Tab. 2 that there is stability for the Nu number when the number of grid elements exceeds the value 115.8000. Therefore, it can be concluded that the second grid G2 is suitable for this research.

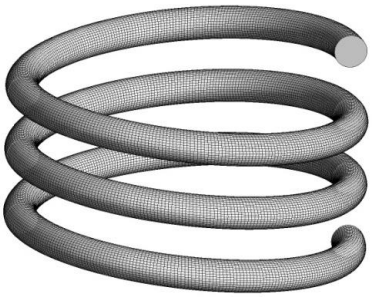

Fig. 2. The structural grid of the studied geometry

Tab. 2. Grid independency test

Grid	Elements	Nu	Difference %
G1	579000	1.478521	2.95
G2	115.8000	1.523521	0.79
G3	2316000	1.511453	–

Nu, Nusselt number

The numerical calculation was done using the finite volume method. This method transforms the differential equations into a matrix system and then solves them using numerical methods. The SIMPLEC algorithm was used for coupling pressure and velocity. However, the high-resolution discretisation scheme was used for solving the convective term.

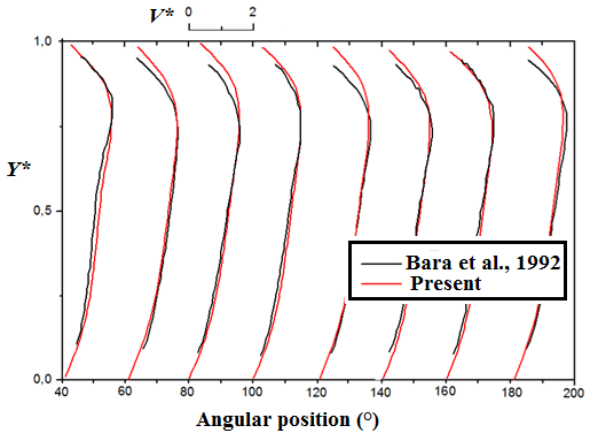

Fig. 3. Comparison of the results of this study with the experimental work of [39]

In addition to this, the accuracy of the results of this method has been proven by comparing the results of this method with the

DOI 10.2478/ama-2022-0014

results of previous works obtained under the same conditions. The first comparison was made with an experiment of the flow inside a curved tube at an angle of 180°. The work was previously done by [39]. Both results are represented in Fig. 3. A very noticeable agreement is found between the results of the experimental and the numerical works. The second comparison was made with the work carried out by [40]. It is a numerical simulation of a fluid in a 180° bent channel of square cross-section. The results of this comparison are represented in Fig. 4. Good agreement is found between the results. Through the results of the comparison study, it is possible to ascertain the effectiveness of this code in arriving at very accurate values.

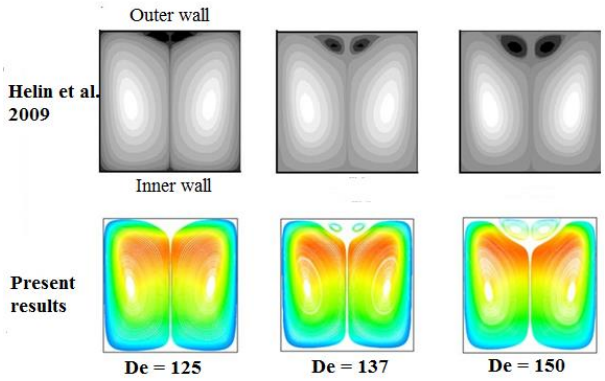

Fig. 4. Comparison of the results of this study with the numerical work of [40]

5. RESULTS AND DISCUSSION

We performed a set of numerical simulations to study a set of factors affecting the behaviour of a complex fluid inside a helical tube. The relevant parameters studied are as follows: the index (*n*),which changes the rheological properties of fluids, takes three values, viz., 0.6, 1 and 1.6; the value of the fluid's velocity determined by the Reynolds number, which varies in the range of 10–600; the intensity of the thermal buoyancy, which is determined by the Richardson number (Ri), which takes the values 0 and 1; and finally, the length of the step between the loops. Accordingly, two values have been tested.

It is worth noting that the analysis of the thermal and dynamic behaviour of the fluid is done by analysing and interpreting the streamlines and the isotherms.Moreover, the mean Nusselt values are presented in the form of curves in terms of the studied pertinent parameters.

5.1. Effect of the Re and Ri numbers

In Figs. 5, 6 and 7, the effects of Ri and Re on the dynamic behaviour of the fluid and its effect on the thermal pattern at $n = 1$ (Newtonian fluid) are presented.

Before we proceed to present the results, we note that the streamlines and isotherms are presented in cross-sections of the angles 90° and –90° together, and the angles 180° and –180° together.

Fig. 5 shows the behaviour of the fluid in the cross-section of angles 90° and -90° for all rings. The behaviour of the fluid is presented in terms of the Re and Ri numbers. It is noticed that when Ri = 0,on increasing the value of the Reynolds number, the flow becomes less stable and the flow is deflected towards the external tube wall. This, of course, is due to the effectof centrifugal force on the flow. The higher the value of Re, the higher is the velocity of the fluid, and this increases the deflection of the flow of the fluid due to the centrifugal force. On the other hand, in the presence of thermal buoyancy force (Ri = 1) effect, two steady vortices appear in this cross-section for Re = 10, but they quickly disappear by raising the value of Re. This phenomenon can be explained as follows: the presence of thermal buoyancy in the opposite direction to the movement of the fluid makes the diameter of the tube smaller, and this raises the seed of the flow in this position (angle 90° and –90°), and accordingly Dean vortices appear.

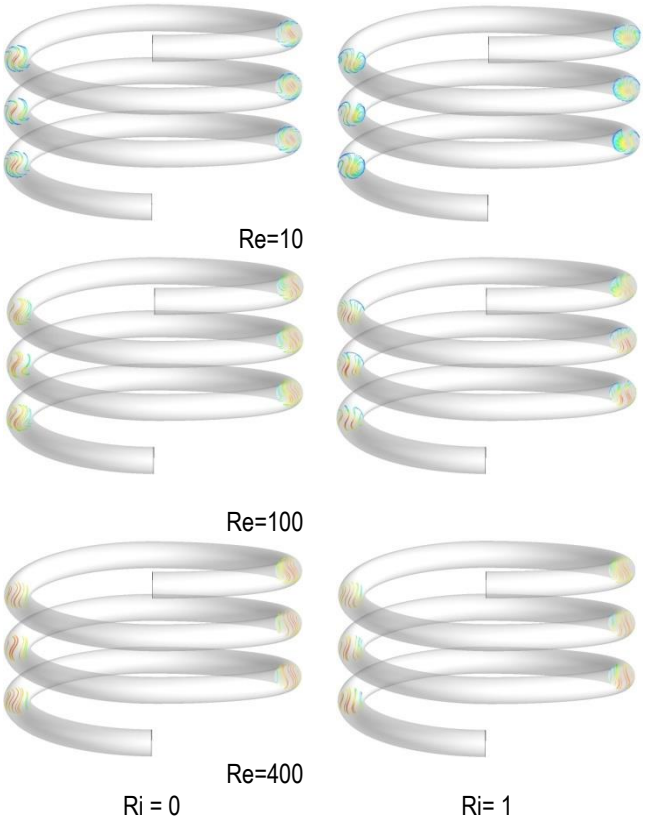

Fig. 5. Streamlines in the cross-sections of the angles 90° and –90° in terms of Re and Ri at $n = 1$ (Re, Reynolds number; Ri, Richardson number)

Fig. 6 shows the same phenomenon, but at the angles 180° and –180°. In this position and in the absence of thermal buoyancy (Ri = 0), the fluid flow is less stable than in the previous positions (angles 90° and –90°), and this is indicated by the presence of Dean vortices in all rings with these angles. It is also noted that the size of these vortices increases with the increase in the value of fluid velocity. In the presence of thermal buoyancy effect (Ri = 1), a slight rotation is observed at the location of the vortices at these angles. This is a result of the transfer of heated particles of the fluid upwards under the influence of thermal buoyancy force.

Fig. 7 shows the isotherms in terms of the studied parameters (Re and Ri) for the angles 90° and –90°. It is noted that the isotherm distribution is not uniform and this is due to the effect of

DOI 10.2478/ama-2022-0014

the centrifugal force on the flow, and from this, it can be deduced that the local heat transfer is different from one point to another. In the first case, i.e. without the effect of thermal buoyancy, it turns out that the outer wall transfers heat with fluid more than the remaining parts of the tube. In the second case, in the presence of thermal buoyancy, it becomes clear that the flow deviates a little to the bottom of the cross-section, making the bottom side more efficient in heat transfer compared to the other sides.

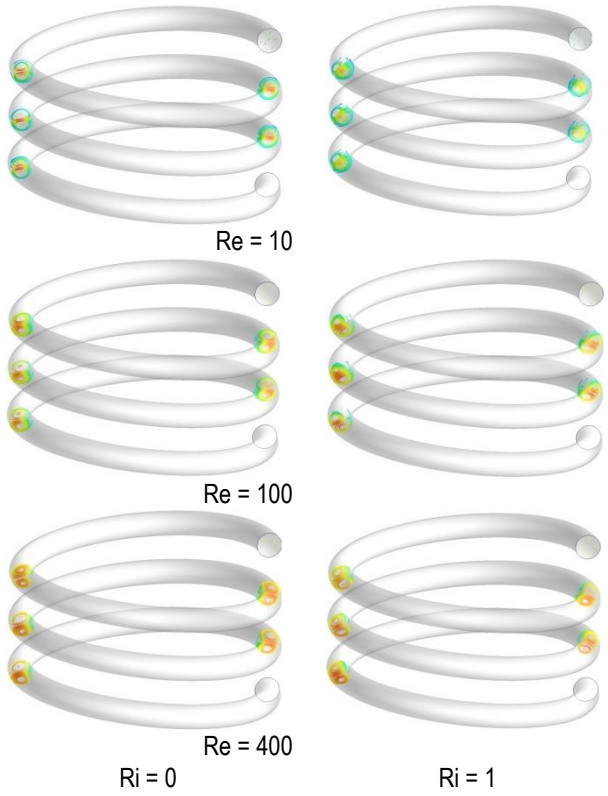

Fig. 6. Streamlines in cross-sections of the angles 180° and –180° in terms of Re and Ri at n = 1 (Re, Reynolds number; Ri, Richardson number)

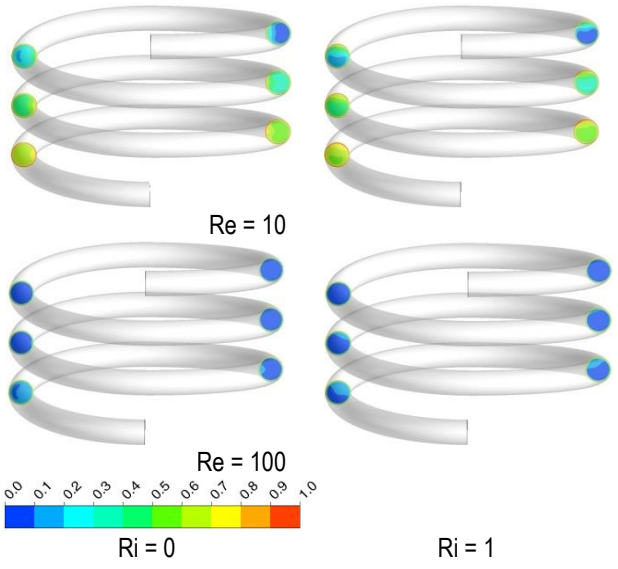

Fig. 7. Isotherms in cross-sections of the angles 90° and –90° in terms of Re and Ri at n = 1 (Re, Reynolds number; Ri, Richardson number)

It can be concluded that the dynamic behaviour of the fluid is affected significantly by the fluid velocity and the intensity of thermal buoyancy.

5.2. Effect of power law index

Through the law of Ostwald, the index n determines the rheological nature of the fluid; therefore, if the value is <1, this means that the fluid is of the shear-thinning type, i.e. a higher fluid velocity leads to a decrease in the viscosity of the fluid. Whereas, if the value of n = 1, the fluid is of the Newtonian type, meaning that the viscosity does not change with the velocity. Whereas, for values of n >1, the viscosity increases its value with velocity and here it is called shear-thickeningfluid. Some examples: blood is a shear-thinning fluid of n is <1; water is a Newtonian fluid of n = 1; chocolate is a shear-thickening fluid of n >1.

Fig.8 shows the distribution of the dimensionless velocity of the flow in the middle of the section of 90° angle in terms of the index n and Ri for Re = 100 and B/D = 0.1. It is noted from Fig. 4 that near the bottom, where the shear stress is very important, the higher the value of the index n, the lower is the fluid velocity, and this is clearly due to the rheological nature of the fluid. On the other hand, it is noted that the thermal effect actually can change the trajectory of the fluid flow.

These curves comprise only a sample, showing the presence of an effect of index n and the number Ri on the behaviour and velocity of fluid flow inside the tube. But this effect changes from one point to another inside the studied tube.

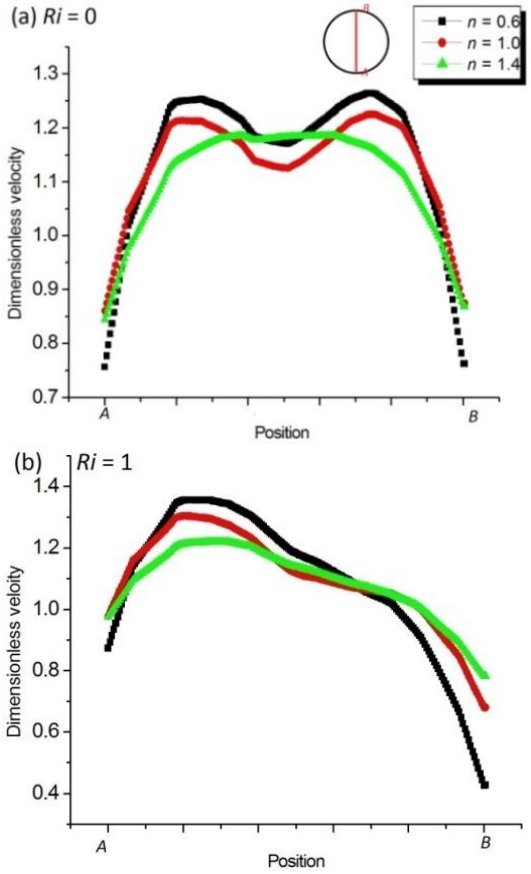

Fig. 8. Distribution of dimensionless velocity along the middle of the cross-section of 90° in terms of n and Ri at Re = 100 Ri, Richardson number.

DOI 10.2478/ama-2022-0014

5.3. Effect of distance between rings

Fig. 9 shows the behaviour of the fluid at the cross-section of angles 180° and –180°for different values of the ratio *B*/*D* and Re at Ri = 1 and *n* = 1. Fig.9 shows the appearance of steady vortices in this section. The shape and size of the vortices are almost not affected by the change of the *B*/*D* ratio, while there is a noticeable development of these vortices in terms of Re in both cases of the *B*/*D* ratio.

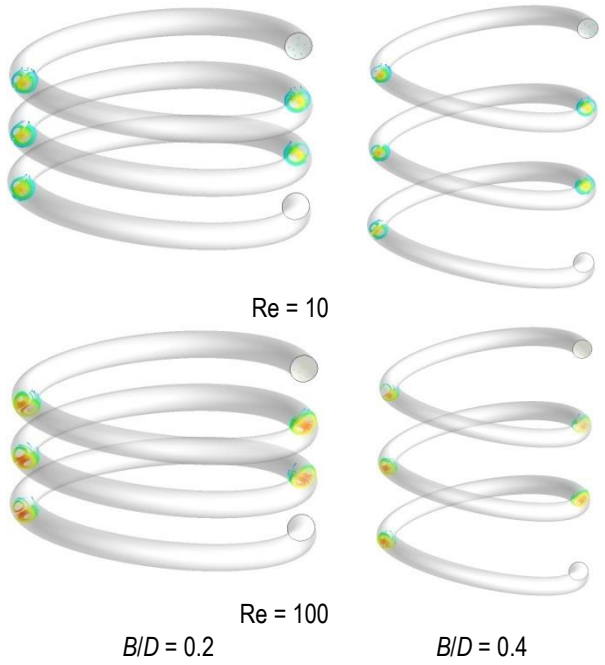

Fig. 9. Streamlines in cross-sections of the angles 180° and –180° in terms of *B*/*D* and Re at *n* = 1 and Ri =1 (B, the pitch between the rings; D, diameter of the tube ring. Re, Reynolds number)

5.4. The average Nusselt number

The main objective of all these studies is to derive the mean values of the Nusselt number in terms of all studied parameters, and accordingly, Fig. 10 explains the changes in the Nu values with *n*, Ri, *B*/*D* and Re. Through Fig. 10, it is shown that the Reynolds number positively affects the values of Nu for all values of *n*, Ri and *B*/*D*. While the changes in the remaining pertinentparameters slightly affect the value of Nu, these changes can be neglected. Finally, it can be concluded that the values of the index n and the number Ri affect the positional distribution of the Nu number, but the average remains approximately the same. In addition to this, the obtained results can be exploited to design helical tube heat exchangers.

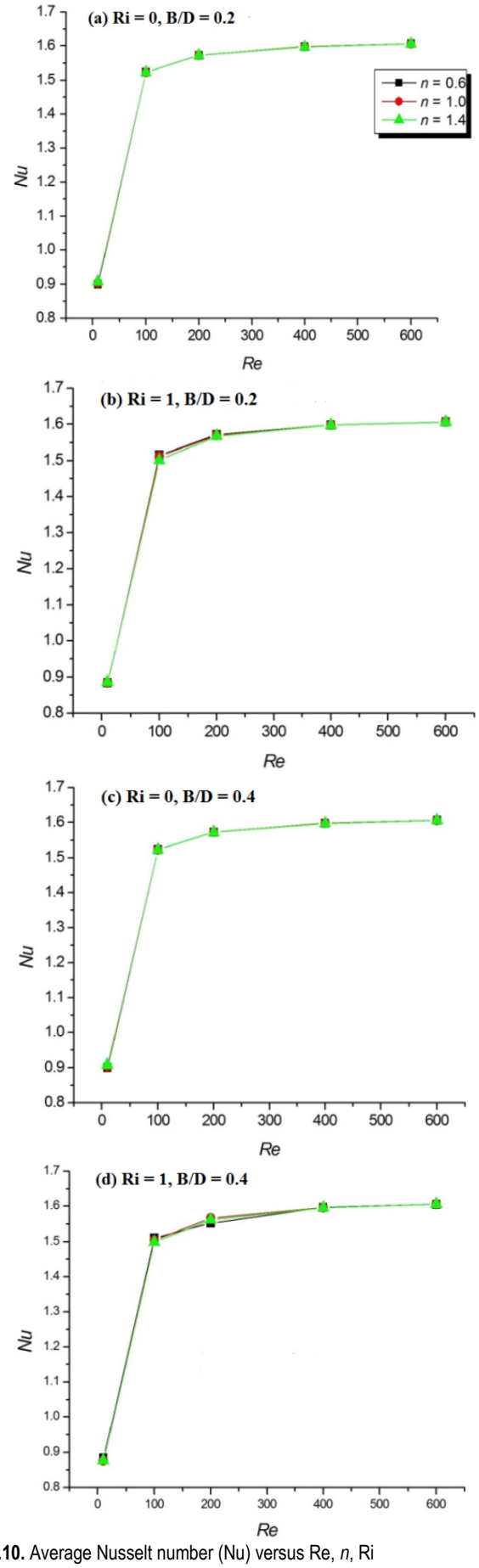

Fig.10. Average Nusselt number (Nu) versus Re, *n*, Ri and *B*/*D* for Pr = 50

6. CONCLUSION

In this work, we studied the dynamic behaviour of a fluid inside a spiral tube and its effect on heat transfer. The fluid used in this research is defined by the Ostwald model. The work was performed numerically in a steady regime. Moreover, the relevant parameters considered are as follows: the Re number (=10–600), the power law index (=0.6, 1 and 1.4), Ri number (=0 and 1) and the pitch ratio (= 0.2 and 0.5). The most important results obtained are summarised as follows:

- The appearance of constant vortices in the cross-section of angles 180° and –180° for all rings and for Ri = 0; the size of the vortices is mainly related to the values of Re.
- For Ri = 1, early vortices appear in the sections for angles 90° and –90°.
- The values of the power law index and Ri affect only the local values of Nu; the mean rate remains approximately the same.
- Raising the values of the flow velocity increases the heat transfer.
- There is no effect of the *B*/*D* ratio on the behaviour of the flow and on the heat transfer for the considered values (0.2 and 0.4).

REFERENCES

1. Ibrahim M, Algehyne EA, Saeed T, Berrouk A S, Chu Y M, Cheraghian G. Assessment of economic, thermal and hydraulic performances a corrugated helical heat exchanger filled with non-Newtonian nanofluid. Scientific Reports. 2021; 11: 11568.
2. Naphon P, Wiriyasart S, Prurapark R, Srichat A. Numerical study on the nanofluid flows and temperature behaviors in the spirally coiled tubes with helical ribs. Case Studies in Thermal Engineering. 2021; 27: 101204.
3. Abu-Hamdeh NH, Alsulami RA, Rawa MJH, Aljinaidi AA, Alazwari M A, Eltaher MA, Almitani KA, Alnefaie KH, Abusorrah AM, Sindi HF, Goodarzi M, Safaei MR. A detailed hydrothermal investigation of a helical micro double-tube heat exchanger for a wide range of helix pitch length. Case Studies in Thermal Engineering. 2021; 28:101413.
4. Abdzadeh B, Hosainpour A, Jafarmadar S, Sharifian F. Thermo-entropic evaluation of the effect of air injection into horizontal helical tube. Journal of Energy Storage. 2021; 38:102542.
5. Zhou C, Yao Y, Ni L. Development of heat transfer correlations for multi-row helically coile d tub e heat exchangers use d in surface water heat pump systems. International Journal of Heat and Mass Transfer. 2020; 163: 120491.
6. Jha VK, Bhaumik SK. Enhanced cooling in compact helical tube cross-flow heat exchanger through higher area density and flow tortuosity. International Journal of Heat and Mass Transfer. 2020; 150: 119270.
7. Zhao H, Li X, Wu Y, Wu X. Friction factor and Nusselt number correlations for forced convection in helical tubes. International Journal of Heat and Mass Transfer. 2020; 155: 119759.
8. Zhou C, Zarrella A, Yao Y, Ni L. Analysis of the effect of icing on the thermal behavior of helical coil heat exchangers in surface water heat pump applications. International Journal of Heat and Mass Transfer. 2022; 183: 122074.
9. Cao Y, Ayed H, Anqi A E, Tutunchian O, Dizaji H S, Pourhedayat S. Helical tube-in-tube heat exchanger with corrugated inner tube and corrugated outer tube: experimental and numerical study. International Journal of Thermal Sciences. 2021; 170: 107139.
10. Ahn K, Lee KH, Lee JS, Won C, Yoon J. Analytic spring back prediction in cylindrical tube bending for helical tube steam generator. Nuclear Engineering and Technology. 2020; 52: 2100-2106.
11. Farnam M, Khoshvaght-Aliabadi M, Asadollahzadeh MJ. Intensified single-phase forced convective heat transfer with helical-twisted tube in coil heat exchangers. Annals of Nuclear Energy. 2021; 154: 108108.
12. Eisapour A H, Naghizadeh A, Eisapour M, Talebizadehsardari P. Optimal design of a metal hydride hydrogen storage bed using a helical coil heat exchanger along with a central return tube during the absorption process. International journal of hydrogen energy. 2021; 46: 14478-14493.
13. Gul S, Erge O, Oort E V. Frictional pressure losses of Non-Newtonian fluids in helical pipes: Applications for automated rheology measurements. Journal of Natural Gas Science and Engineering. 2020; 73: 103042.
14. Gul S, Erge O, Oort E V. Helical Pipe Viscometer System for Automated Mud Rheology Measurements. IADC/SPE International Drilling Conference and Exhibition. 2020; IADC/SPE-199572-MS.
15. Mokeddem M, Laidoudi H, Bouzit M. 3D Simulation of Dean vortices at 30 position of 180 curved duct of square cross-section under opposing buoyancy. Defect and Diffusion Forum. 2018; 389: 153-163.
16. Mokeddem M, Laidoudi H, Makinde OD, Bouzit M. 3D Simulation of incompressible poiseuille flow through 180° curved duct of square cross-section under effect of thermal buoyancy. Periodica Polytechnica Mechanical Engineering. 2019; 63: 257-269.
17. Mokeddem M, Laidoudi H, Bouzit M. Computational Analyses of Flow and Heat Transfer at 60° Position of 180° Curved Duct of Square Cross-Section. Diffusion Foundations. 2020; 26: 53-62.
18. Cao X, Du T, Liu Z, Zhai H. Experimental and numerical investigation on heat transfer and fluid flow performance of sextant helical baffle heat exchangers. International Journal of Heat and Mass Transfer. 2019; 142: 118437.
19. Cao X, Chen D, Du T, Liu Z, Ji S. Numerical investigation and experimental validation of thermo-hydraulic and thermodynamic performances of helical baffle heat exchangers with different baffle configurations. International Journal of Heat and Mass Transfer. 2020; 160: 120181.
20. Chen Y, Tang H, Wu J, Gu H, Yang S. Performance comparison of heat exchangers using sextant/trisection helical baffles and segmental ones. Chinese Journal of Chemical Engineering. 2019; 27: 2892–2899.
21. Chen D, Zhang R, Cao X, Chen L, Fan X. Numerical investigation on performance improvement of latent heat exchanger with sextant helical baffles. International Journal of Heat and Mass Transfer. 2021; 178: 121606.
22. Jamshidi N, Mosaffa A. Investigating the effects of geometric parameters on finned conical helical geothermal heat exchanger and its energy extraction capability. Geothermics. 2018; 76: 177–189.
23. Abu-Hamdeh NH, Almitani KH, Alimoradi A. Exergetic performance of the helically coiled tubeheat exchangers: Comparison the sector-by-sector with tube in tube types. Alexandria Engineering Journal. 2021; 60: 979–993.
24. Abu-Hamdeh NH, Bantan RAR, Tlili I. Analysis of the thermal and hydraulic performance of the sector-by-sector helically coiled tube heat exchangers as a new type of heat exchangers. International Journal of Thermal Sciences. 2020; 150: 106229.
25. Liu S, Huang W, Bao Z, Zeng T, Qiao M, Meng J. Analysis, prediction and multi-objective optimization of helically coiled tube-in-tube heat exchanger with double cooling source using RSM. International Journal of Thermal Sciences. 2021; 159: 106568.
26. Mirgolbabaei H. Numerical investigation of vertical helically coiled tube heat exchangers thermal performance. Applied Thermal Engineering. 2018; 136: 252–259.
27. Javadi H, Ajarostaghi S S M, Pourfallah M, Zaboli M. Performance analysis of helical ground heat exchangers with different configurations. Applied Thermal Engineering. 2019; 154: 24–36.
28. Maghrabie H M, Attalla M, Mohsen AAA. Performance assessment of a shell and helically coiled tube heat exchanger with variable orientations utilizing different nanofluids. Applied Thermal Engineering. 2021; 182: 116013.

29. Vivekanandan M, Venkatesh R, Periyasamy R, Mohankumar S, Devakumar L. Experimental and CFD investigation of helical coil heat exchanger with flower baffle. Materials Today: Proceedings. 2021; 37: 2174–2182.
30. Sadhasivam C, Murugan S, Manikandaprabu P, Priyadharshini SM, Vairamuthu J. Computational investigations on helical heat flow exchanger in automotive radiator tubes with computational fluid dynamics, Materials Today : Proceedings. 2021; 37: 2352–2355.
31. Gokulnathan E, Pradeep S, Jayan N, Bhatlu M L D, Karthikeyan S. Review of heat transfer enhancement on helical coil heat exchanger by additive passive method, Materials Today. Proceedings. 2021; 37: 3024–3027.
32. Padmanabhan S, Reddy OY, Yadav KVAK, Raja VKB, Palanikumar K. Heat transfer analysis of double tube heat exchanger with helical inserts, Materials Today: Proceedings. 2021; 46: 3588–3595.
33. Naik B, Hosmani A K, Kerur S M, Jadhav CC, Benni S, Annigeri S, Javali T, Aralikatti P. Numerical analysis of two tube helical heat exchanger using various nano-fluids, Materials Today: Proceedings. 2021; 47: 3137–3143.
34. Kumar PCM, Chandrasekar M. CFD analysis on heat and flow characteristics of double helically coiled tube heat exchanger handling MWCNT/water nanofluids. Heliyon. 2019; 5: e02030.
35. Dhumal G S, Havaldar SN, Numerical investigation of heat exchanger with inserted twisted tape inside and helical fins on outside pipe surface. Materials Today. Proceedings. 2021; 46: 2557–2563.
36. Kareem R. Optimisation of Double Pipe Helical Tube Heat Exchanger and its Comparison with Straight Double Tube Heat Exchanger. J. Inst. Eng. India Ser. C. 2017; 98, 587–593.
37. Zainith P, Mishra N K. Heat Transfer Enhancement of Al2O3-Based Nanofluid in a Shell and Helical Coil Heat Exchanger.Advances in Applied Mechanical Engineering. Lecture Notes in Mechanical Engineering. 2020. https://doi.org/10.1007/978-981-15-1201-8_18
38. Miansari M., Jafarzadeh A., Arasteh H. and Toghraie D. (2021), Thermal performance of a helical shell and tube heat exchanger without fin, with circular fins, and with V-shaped circular fins applying on the coil, Journal of Thermal Analysis and Calorimetry,143, 4273–4285.
39. Bara B, Nandakumar K, Masliyah J H. An experimental and numerical study of the Dean problem: flow development towards two-dimensional multiple solutions. Journal of Fluid Mechanics. 1992; 244: 339–376.
40. Helin L, Thais L, Mompean G. Numerical simulation of viscoelastic Dean vortices in a curved duct. Journal of Non-Newtonian Fluid Mechanics. 2009; 156: 84–94.

Mohamed Ramla: https://orcid.org/0000-0002-7144-5264

Houssem Laidoudi: https://orcid.org/0000-0001-8700-7077

Mohamed Bouzit: https://orcid.org/0000-0002-1417-7291